Characterization and toxicity of a phosphate-binding exobiopolymer produced by *Acinetobacter haemolyticus* MG606

Taranpreet Kaur and Moushumi Ghosh

ABSTRACT

A novel, phosphate-binding exobiopolymer (EBP) produced by *Acinetobacter haemolyticus* MG606 was characterized and its biocompatibility evaluated in RAW 264.7 cells and in mice. EBP was identified as a 50 kDa heteropolysaccharide composed of pentose and hexose sugars. EBP exhibited cytotoxicity, stimulation of free radical production and loss of mitochondrial and lysosomal integrity in RAW 264.7 cells at 500 μg/mL concentration while lower concentrations exhibited no significant ($p > 0.05$) effect on these parameters. EBP exhibited dose-dependent mortality, body weight reduction, hypothermia and clinical signs of toxicity in mice following intraperitoneal administration. The LD_{50} of EBP was determined to be 92.31 mg/kg. Overall, the results of our study suggest that composition of EBP produced by *A. haemolyticus* MG606 is distinct from EBP produced by other *Acinetobacter* spp. The high biocompatibility supports application of EBP as a safe biosorbent for phosphate remediation.

Key words | *Acinetobacter haemolyticus*, characterization, exobiopolymer, toxicity

Taranpreet Kaur
Moushumi Ghosh (corresponding author)
Department of Biotechnology,
Thapar University,
Patiala 147 004,
India
E-mail: *mghosh@thapar.edu*

HIGHLIGHTS

- *Acinetobacter haemolyticus* MG606 produces a 50 kDa heteropolysaccharide;
- EBP exhibits *in vitro* toxicity and free radical production at high concentrations;
- Mitochondrial and lysosomal damage is apparent at high EBP concentrations;
- EBP exhibits dose-dependent toxicity in mice;
- LD_{50} of EBP following intraperitoneal administration in mice is 92.31 mg/kg.

INTRODUCTION

Bioremediation of anthropogenic pollutants using natural polymers has received immense interest over the past decades. Several polymers of microbial and plant origin have been recognized as potential bioremediants for adsorptive removal of heavy metals and organic contaminants (Nguyen *et al.* 2012; More *et al.* 2014). However, in striking contrast to research on bioremediants for highly toxic compounds, bioremediation methods for inorganic anions are still in infancy (More *et al.* 2014).

Phosphate is one of the most important anionic pollutants which has attracted attention in recent years. Phosphate is generally present in small amounts in natural waters. However, its ever increasing agricultural usage coupled with escalating discharges from household and poultry wastes has resulted in augmentation of phosphate levels in freshwater bodies. The accumulation of phosphate in lakes and estuaries is a prerequisite for and a cause of algal blooms, culminating in eutrophication (Rockstrom *et al.* 2009; UNEP 2012). Few reports exist on phosphate

doi: 10.2166/wh.2016.176

bioremediation using microbial exobiopolymers (EBP) and plant-derived polymers (Yang *et al.* 2011; Riahi *et al.* 2014). However, the practical applicability of these biopolymers is compromised by two important constraints: first, phosphate-binding capacity of these polymers is in the range of 2–10 mg phosphate/g polymer which is too low for commercially viable applications. The low adsorption efficiency of pristine polymers could be augmented by functionalization with metals but this approach is limited by high production costs and leeching of metal ions during sorbent recovery (Nguyen *et al.* 2015). The second constraint is the toxicity/biocompatibility of these polymers is largely unknown. Biopolymers are generally considered safe due to their polysaccharide nature and this caveat forms the basis for a dearth of systematic toxicity studies (Ramberg *et al.* 2010). Nonetheless, this generalization is void since biopolymer structure and composition exhibit significant interstrain differences even in members of the same species. These structural and compositional differences transform into divergence in physicochemical properties and toxicological profiles (Ruas-Madiedo *et al.* 2010). A precise knowledge of toxicological profile is important to determine human and environmental safety, safe exposure levels during manufacturing, methods of disposal and countermeasures to be undertaken during accidental leakage.

Our group has earlier reported the high affinity binding of phosphate with Acinetobacter EBP with possible applications in environmental monitoring (Kaur *et al.* 2013a, 2013b). In a recent report, we have also reported phosphate removal in batch equilibrium studies and proposed a mechanism of phosphate binding (Kaur & Ghosh 2015). In the current study, we report further characterization of EBP and its toxicity in a macrophage cell line and mouse lethality assay.

MATERIAL AND METHODS

Chemicals and media

All chemicals and media components used were purchased either from HiMedia (India) or other suppliers and were of the highest purity available.

Strain and culture conditions

Acinetobacter haemolyticus MG606 was grown in nutrient broth for routine subculturing. The strain was transferred to EBP production medium for extraction of EBP as described earlier (Kaur & Ghosh 2015).

Characterization of EBP

Molecular weight was determined by gel permeation chromatography using Sephacryl S-300 column and eluted with 0.1 M NaCl. The eluting fractions were manually collected and retention volume calculated. The molecular weight was calculated from retention volume by comparison with retention volume of dextran standards of different molecular weights (Badrinathan *et al.* 2012).

Monosaccharide composition was determined by aldol-acetate method. Briefly, EBP was hydrolyzed with 2 M trifluoroacetic acid and the liberated monosaccharides were converted to aldol-acetate by sequential treatment with sodium borohydride and pyridine/acetic anhydride. The derivatized monosaccharides were analyzed by gas chromatography mass spectrometry (GCMS). Linkage analysis was performed by methylation analysis (Bales *et al.* 2013). The partially methylated aldol acetates were determined by GCMS as described above.

Fourier transform infrared (FTIR) spectrum was recorded by the potassium bromide pellet method (Kaur & Ghosh 2015). FTIR spectrum was deconvoluted using PeakFit software.

Cells and culture medium

Mouse macrophage cell line (RAW 264.7) was maintained according to standard methods (Singh *et al.* 2013). Briefly, RAW 264.7 cells (National Centre for Cell Sciences, Pune, India) were maintained in Dulbecco's modified Eagle's medium (DMEM) containing 10% fetal bovine serum (FBS). The flasks were incubated at 37 °C until confluent and then trypsinized. The cell suspension was seeded in T75 flasks for subculturing. All culture components were obtained from HiMedia, India.

In vitro toxicity

Confluent cultures were trypsinized and cell number was counted on a haemocytometer. The cell suspension was adjusted to 5×10^4 cells/mL with DMEM containing 10% FBS and 0.2 mL of cell suspension was seeded in 96 well plates. The plates were incubated overnight for cell attachment and culture medium was then replaced with culture medium containing EBP (100–500 μg/mL) or culture medium (untreated control). Following 24 hours incubation, culture medium was replaced with 0.2 mL DMEM containing MTT (0.5 mg/mL). Cell viability was calculated from the amount of formazon produced and expressed as percentage of untreated control (Singh *et al.* 2013).

Cellular activation was determined by monitoring stimulation of reactive oxygen species (ROS) and nitrite production by dichlorofluorescein (DCF) method and Greiss reaction, respectively. Mitochondrial and lysosomal integrity was determined by safranin O and neutral red uptake, respectively (Singh *et al.* 2013).

Animals

Female Swiss mice weighing 20–30 g and aged 8–12 weeks old were acclimatized to 22 ± 3 °C; 30–70% relative humidity and 12 hour light/dark cycle for 7 days before commencing experimentation. These laboratory conditions were also maintained during the course of experimentation. Food and water were provided *ad libitum* during the entire course of study. All animal experimentation was performed at Venus Medicine Research Centre, Baddi, India.

In vivo toxicity

Precalculated amounts of EBP were separately dissolved in pyrogen-free saline to administer doses ranging from 60 to 140 mg/kg EBP. The EBP solutions of different concentrations were injected intraperitoneally to administer indicated doses. The dose range was selected on the basis of a preliminary sighting study performed with a wider dose range (data not shown). Body weight, rectal temperature, clinical signs of toxicity and mortality were observed for 7 days after administration of a single dose of EBP. Gross necropsy was performed on the same day in animals that died during study and on day 7 in all surviving animals.

Statistical analysis

The dye absorbance (MTT formazon, safranin O and neutral red) and fluorescence intensity (DCF) in untreated cells (control) was considered 100% and absorbance in EBP-treated cells was converted to percentage of control. The data for all *in vitro* and *in vivo* parameters were converted to mean ± SD. The intergroup differences were compared by one-way analysis of variance (ANOVA) followed by Tukey's test.

RESULTS AND DISCUSSION

Characterization of EBP

Size separation of polysaccharide fraction revealed a single polysaccharide component with a molecular weight of approximately 50 kDa. Monomer composition revealed the heteropolysaccharide nature of EBP with relative monosaccharide proportion of glucose:xylose:arabinose:ribose:galactose:allose:lyxose 3:2:2:2:2:2:1. Additionally, small amounts of mannose (approximately 5%) were also detected. Monosaccharide composition of *A. haemolyticus* MG606 EBP determined by aldol-acetate method is in agreement with previously reported composition determined by silylation method (Kaur & Ghosh 2015).

Vibrational spectroscopy of 'anomeric region' (950–750 cm^{-1}) and 'sugar region' (1,200–950^{-1}) of FTIR spectrum provide valuable information on polysaccharide structure. FTIR spectrum of EBP revealed a high intensity peak at 1,032 cm^{-1} and low intensity peak at 875 cm^{-1}. In case of fungal EBP, peaks at ca. 1,160, 1,078, 1,041 and 889 cm^{-1} have been attributed to the presence of (1,3)- and/or (1,6)-linked β-glucans while peaks at ca. 1,155, 1,023, 930, 850 and 765 cm^{-1} have been attributed to (1,4)- and/or (1,6)-linked α-glucans (Sandula *et al.* 1999). The presence of features at 1,032 and 875 cm^{-1} along with absence of peaks at 930 and 765 cm^{-1} therefore, suggests that (1,3)- and/or (1,6)-linked β-glucans constitute the major fraction. The features at 1,160 and 1,078 cm^{-1} were not discernible due to a broad shoulder with peak at

1,032 cm^{-1}. Therefore, the peaks in this region were resolved by deconvolution of FTIR spectrum. Deconvolution of peaks revealed presence of an additional peak at 1,072 cm^{-1} further confirming presence of (1,3)- and/or (1,6)-linked β-glucans in EBP (Figure 1).

GCMS of methyl glycosides revealed the presence of 2-, 3-, 4/5- and 6-linked hexoses as well as 2,4-, 2,6-, 3,6-, 4,6-linked hexoses. Similarly, 2-, 3- and 4/5-linked pentoses were also detected along with 2,4-, 3,4- and 3,5-linked hexoses. It is worth mentioning here that pyranose and furanose forms isomerize during acid methanolysis and hence, a distinction between 4- and 5-linked sugars was not possible. Further, high proportions (>25%) of tri-linked (1,2,4-, 1,2,3-, 1,2,5-, 1,2,6-, etc.) and tetra-linked (1,2,3,4-, 1,2,4,6-, etc.) along with unmethylated monosaccharides (<5%) were detected. Based on existing literature on microbial EBPs, it is highly unlikely that tetra-linked monosaccharides could be present in such high proportions in EBP. The detection of unmethylated along with tetra-linked monosaccharides suggest the possibility of undermethylation of EBP, presumably due to low solubility in solvent (dimethylsulfoxide) (Laine *et al.* 2002). This precluded a reliable quantitative estimation of different linkages in EBP and hence, the results obtained are not shown. Nonetheless, despite these shortcomings, a qualitative analysis of different linkages was still pragmatic and validated the presence of (1,3)- and (1,6)-linked sugars as determined from FTIR studies.

Acinetobacter genus comprises of 27 species (Peleg *et al.* 2012), however, EBP produced by only three named species (*A. baumanni*, *A. calcoaceticus* and *A. junii*) and one unnamed species (Acinetobacter sp. 12S) have been characterized (Pirog *et al.* 2009; Bales *et al.* 2013; Sen *et al.* 2014). Recently, we have reported that *A. haemolyticus* produces EBP with chemical characteristics significantly different from other Acinetobacter EBPs (Kaur & Ghosh 2015). The most distinctive feature of *A. haemolyticus* MG606 was the presence of pentose sugars in very high proportions which were either not detected or were present in minuscule amounts in EBPs produced by other Acinetobacteria. The linkage pattern of hexoses in *A. haemolyticus* MG606 EBP is similar to that observed in other Acinetobacter sp. (Satpute *et al.* 2010; Bales *et al.* 2013).

In vitro toxicity

EBP did not alter cell viability at concentrations up to 400 μg/mL in RAW 264.7 cells while a significant reduction in cell viability was observed at 500 μg/mL EBP (Figure 2). The *in vitro* toxicity was further confirmed by morphological evaluation of cells exposed to EBP. Cellular morphology remained unaltered up to 400 μg/mL EBP while rounding and detachment of cells was observed at 500 μg/mL, thus supporting observations in cell viability assay (Figure 3). A similar degree of *in vitro* toxicity has also been demonstrated in natural and modified starch, cellulose and chitosan as well as plant polysaccharides, dextran sulfate and curdlan, thus confirming biocompatibility of EBP (Kean & Thanou 2010). Cellular activation is the first line of non-specific defense mounted by macrophages in response to foreign particles and macromolecules. As a

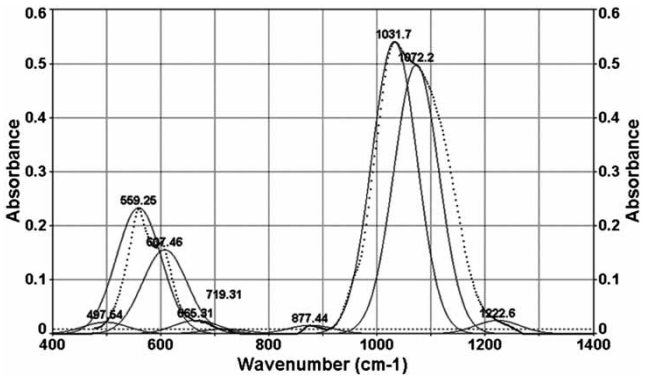

Figure 1 | FTIR spectrum of EBP. Dotted line shows the actual spectrum and solid lines show the peaks identified by deconvolution.

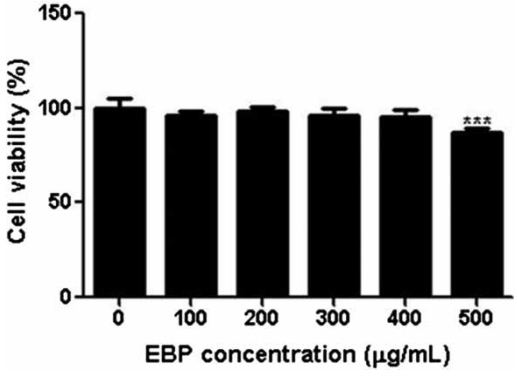

Figure 2 | Effect of EBP on viability of RAW 264.7 cells after 24 hours incubation. Data are mean ± SD of two experiments run in triplicate. ***$p < 0.001$ compared to control.

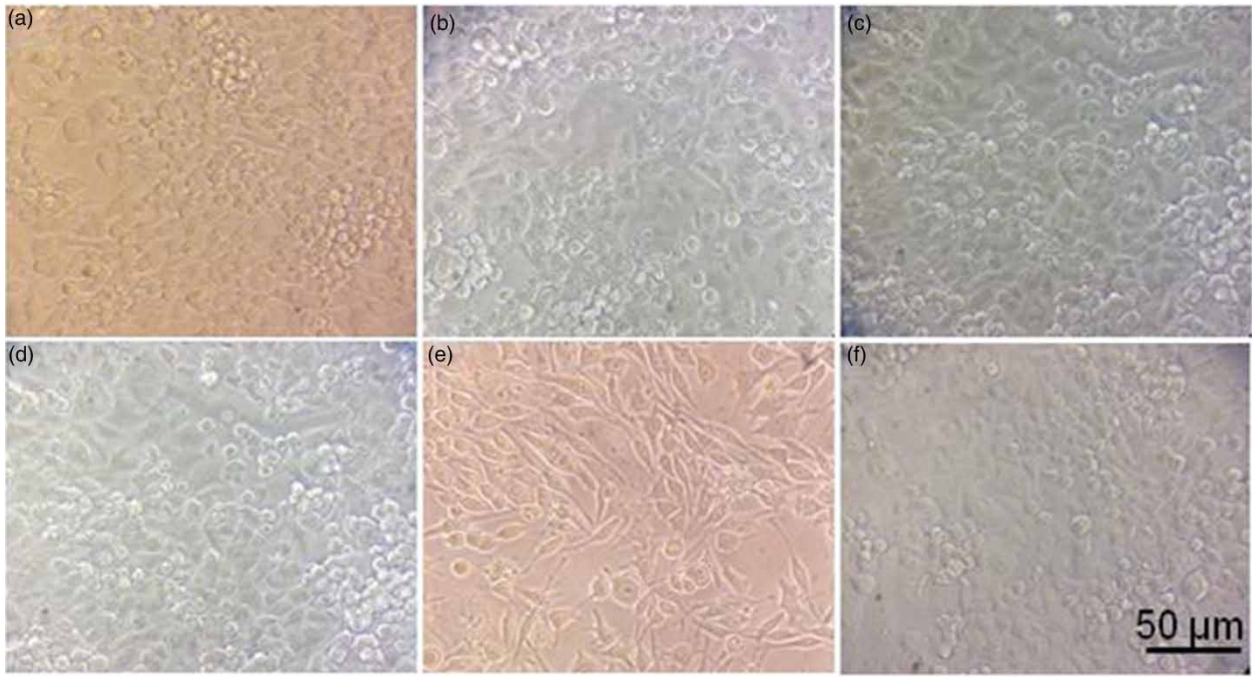

Figure 3 | Effect of EBP on morphology of RAW 264.7 cells after 24 hours incubation. (a) Untreated control (0 μg/mL EBP), (b) 100 μg/mL EBP, (c) 200 μg/mL EBP, (d) 300 μg/mL EBP, (e) 400 μg/mL EBP, (f) 500 μg/mL EBP.

consequence of this activation, free radical production is augmented which further activates other cellular cascades involved in host defense (Brune *et al.* 2013). Under conditions of continuous stimulation, free radical production may also trigger cell death pathways by destabilization of mitochondrial and lysosomal membranes (Terman *et al.* 2006; Meyer *et al.* 2013). Therefore, the effect of EBP on free radical production as well as mitochondrial and lysosomal integrity was determined.

ROS production in RAW 264.9 cells remained unaltered up to 400 μg/mL EBP while a significant increase, as evident by an increase in DCF fluorescence, was observed at 500 μg/mL EBP. A similar trend was also observed for nitrite production whereby nitrite production was stimulated only at the highest concentration (500 μg/mL EBP) in RAW 264.7 cells (Figure 4). Mitochondrial and lysosomal integrity was partially lost at 500 μg/mL EBP while no effect was observed at lower concentrations (Figure 4). These results are in agreement with the results of cell viability assay, suggesting high biocompatibility. The observed activation of RAW 264.7 cells, as evident from the augmentation of ROS and nitrite production, is commensurate with immunomodulatory properties of microbial and plant polysaccharides (Ramberg *et al.* 2010).

In vivo toxicity

Systemic administration (i.p.) of EBP in mice ($n = 4$/group) resulted in dose-dependent mortality. No mortality was observed at the lowest dose (60 mg/kg) while 25, 75, 75 and 100% mortality was observed at dose levels of 80, 100, 120 and 140 mg/kg, respectively, within 2 hours of EBP administration. Gross necropsy of dead animals revealed petechial to ecchymotic hemorrhages in heart, kidney and liver. No further mortalities were observed over a period of 7 days and gross necropsy revealed no pathological changes in animals that survived until study completion (7 days post-administration). The value of LD_{50} was determined to be 92.31 mg/kg. The LD_{50} of EBP was comparable to LD_{50} of high molecular weight dextran sulphates (0.1–0.5 mg/kg), neutral mannan present in baker's yeast (75 mg/kg) and carrageenan (5,000–9,150 mg/kg) (Nagase *et al.* 1984; CIR 2012; Necas & Bartosikova 2013). The proximity of LD_{50} values of EBP with

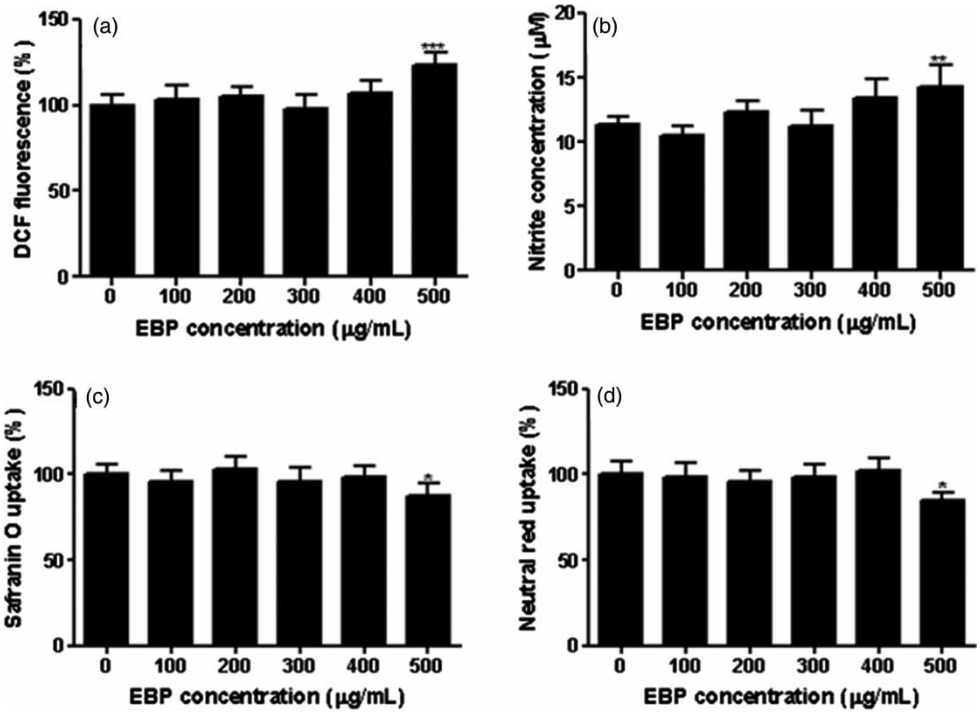

Figure 4 | Effect of EBP on ROS production (a), nitrite production (b), mitochondrial integrity (c) and lysosomal integrity (d) in RAW 264.7 cells after 24 hours incubation. Data in (a), (c) and (d) are normalized to dye intensity in control cells and expressed as percentages relative to control cells. Data in (b) represent nitrite levels in culture supernatants. Data are mean ± SD of two experiments run in triplicate. *$p < 0.05$, **$p < 0.01$, ***$p < 0.001$ compared to control.

polysaccharides used in pharmaceuticals (dextrans) and present in food (yeast neutral mannan) support the biocompatability of EBP. The low *in vivo* toxicity is also in consonance with the observed low *in vitro* toxicity in RAW 264.7 cells, thereby validating high biocompatibility of EBP.

Mortality and changes in organ appearance (gross necropsy) represent extreme toxicological outcomes whereby the toxicity is significant enough to manifest itself as organ damage, culminating in death. Although suitable for preliminary investigations, these endpoints have generally been criticized due to their low sensitivity and non-specificity. Another drawback of these endpoints is that they provide little or no information on the mechanism of toxicity. Therefore, additional endpoints are generally recommended which are more sensitive and provide subtle clues about possible mechanisms of toxicity. These endpoints include changes in body weight, body temperature and clinical signs of toxicity (Iezhitsa *et al.* 2002).

Daily body weights were recorded from the day of EBP injection until study termination (day 7). Comparative analysis of body weights between all observation days revealed no significant ($p > 0.05$; F value 0.149) changes in body weights when treated with 60 mg/kg of EBP while a significant difference in body weight was observed at 80 mg/kg of EBP treatment on the 6th and 7th day ($p < 0.05$; F value 3.048). The average body weight was reduced by 1.5 and 10.1% on day 7 compared to initial body weights (day 0) in 60 and 80 mg/kg treatment groups, respectively. Similarly, the average body weight was reduced by 14.5 and 13.8% in 100 and 120 mg/kg groups, respectively, while body weights could not be recorded in the 140 mg/kg group due to treatment-related mortality in all animals. Further, statistical comparison of body weights could not be performed in the 100, 120 and 140 mg/kg groups since the sample size was too small ($n < 2$) due to treatment-related mortalities within 2 hours of EBP administration (Table 1).

Rectal temperatures were recorded at study initiation (0 min) and then at 30, 60, 90, 120, 180, 240 and 480 min. The range of rectal temperature at 0 min was 35.8 ± 1 °C. No change in rectal temperature was observed at the

Table 1 | Mean body weights of mice injected with single dose of EBP at different dose levels

	Days							
Dose (mg/kg)	**0**	**1**	**2**	**3**	**4**	**5**	**6**	**7**
60	33.8 ± 1.7	33.5 ± 1.7	33.5 ± 1.3	33.5 ± 1.7	32.8 ± 2.2	32.8 ± 2.5	33.3 ± 1.7	33.3 ± 1.5
80	33.0 ± 1.8	32.0 ± 1.0	31.0 ± 1.0	31.3 ± 1.5	30.3 ± 1.5	30.7 ± 1.2	30.0 ± 1.0	29.7 ± 0.6
100	32.8 ± 1.0	31.0 ± NA[a]	30.0 ± NA[a]	30.0 ± NA[a]	29.0 ± NA[a]	29.0 ± NA[a]	28.0 ± NA[a]	28.0 ± NA[a]
120	32.5 ± 0.6[a]	31.0 ± NA[a]	31.0 ± NA[a]	29.0 ± NA[a]	29.0 ± NA[a]	28.0 ± NA[a]	29.0 ± NA[a]	28.0 ± NA[a]
140	32.3 ± 1.7	NR[b]	NR[b]	NR[b]	NR[b]	NR[b]	NR[b]	NR[b]

Data represent mean ± SD of surviving animals ($n = 4$/group on day 0).
[a]Not applicable (NA); only one animal survived.
[b]Not recorded (NR) as all animals died.

lowest dose (60 mg/kg) during the 480 min observation period. One animal in the 80 mg/kg EBP group exhibited a 2 °C fall in body temperature after 30 min and subsequently died with 1 hour of treatment. No other animal in this group exhibited hypothermia. All animals ($n = 4$) in the next higher dose group (100 mg/kg) exhibited marked hypothermia (>1.9 °C) after 30–60 min post-administration. Three animals of this group died within 30 min of induction of hypothermia while one animal recovered from hypothermia and survived until study termination (day 7). Similarly, one animal died of hypothermia after 60 min while one animal recovered from hypothermia and survived until study termination. Two additional animals in the 120 mg/kg group and all animals in the 140 mg/kg group died within 30 min of EBP administration and hence, rectal temperatures could not be recorded at 30 min. Nonetheless, it is plausible to assume that these animals which died within 30 min of EBP administration could have also exhibited hypothermia considering the general trend in the lower dose group (100 mg/kg EBP) and the observed hypothermia in two animals of the 120 mg/kg group. A similar hypothermic response has also been reported following the administration of toxins and toxic chemicals in rodents (Ismail *et al.* 1990).

Clinical signs of toxicity were recorded through the duration of study. A complete list of all parameters is provided in Table 2. The frequency and intensity of adverse effects exhibited a dose-dependent pattern. Apart from

Table 2 | List of clinical signs of toxicity

1. No abnormality detected	9. Irritable animal	17. Nasal discharge	25. Pupil size changed	33. Prostration (exhausted and collapsed)
2. Dull/Lethargic animal	10. Diarrhea	18. Weak grip strength	26. Lack of interest in food	34. Restless/Hyperactive animal
3. Body weak and emaciated	11. Increased preening	19. Swollen eyes	27. Bizarre behavior	35. Nonresponsive to external stimuli
4. Presence of tremor	12. Unsteady gait	20. Red eyes	28. Dry/Dirty furcoat	36. Pyrexia
5. Decreased grasp or hold	13. Panting/ Gasping	21. Increased blinking	29. Dull/Lustureless furcoat	37. Avoiding light (photophobia)
6. Drowsy or sleepy animal	14. Loss of hair	22. Vomiting	30. Repetitive circling	38. Unusual respiration pattern
7. Lacrimation	15. Laboured breathing	23. Dead animal	31. Abnormal gait pattern	39. Hunched back posture and shrunken flanks
8. Pilo-erection	16. Edema	24. Erythema	32. Bleeding from paw or tail	40. Decreased blinking (staring look) 41. Hypothermia) 42. Others (if any)

Table 3 | Clinical signs of toxicity observed in animals that died during study and that survived until day 7

		Days							
Dose (mg/kg)	**Animal condition[a]**	**0**	**1**	**2**	**3**	**4**	**5**	**6**	**7**
60	Live (4)	1	1, 8	1, 8	1	1	1	1	1
80	Live (3)	1	4, 5, 8, 18, 29, 39, 41, 23	23	23	23	23	23	23
	Dead (1)	1	8, 18, 29	29	29	1	1	1	1
100	Live (1)	1	8, 18, 41	8, 18, 41	8	8	8	1	1
	Dead (3)	1	4, 5, 8, 18, 29, 39, 41, 23	23	23	23	23	23	23
120	Live (1)	1	8, 18, 41	8, 18, 41	8, 18, 41	8, 18	8	8	8
	Dead (3)	1	4, 5, 8, 18, 29, 39, 41, 23	23	23	23	23	23	23
140	Live (0)	1	–	–	–	–	–	–	23
	Dead (4)	1	4, 5, 8, 18, 29, 39, 41, 23	23	23	23	23	23	23

[a]Animal condition indicates animals that survived until day 7 (live) and that died during the course of study. Numbers in parentheses indicate number of live/dead animals ($n = 4$/group on day 0).

hypothermia and death as discussed above, other signs of toxicity observed were tremors, decreased grasp/hold, piloerection, weak grip strength, dull furcoat and hunched posture with shrunken flanks. The clinical signs of toxicity observed in animals that died during the study and those which survived are shown in Table 3.

CONCLUSIONS

EBP was identified as a 50 kDa heteropolysaccharide composed of pentose and hexose sugars. The *in vitro* toxicity of EBP was apparent at high concentration and comparable to several commercially important polysaccharides, thus indicating the biocompatible nature of EBP. The LD_{50} of EBP in mice was determined to be 92.31 mg/kg which is in close agreement with other, commercially important polysaccharides. The *in vivo* results complemented observations in *in vitro* studies and confirmed the high biocompatibility of EBP. The high biocompatibility supports the application of EBP as a safe biosorbent for phosphate remediation.

ACKNOWLEDGEMENTS

This work was supported by a grant from University Grants Commission (UGC), India. TK received Maulana Azad National Fellowship from UGC.

REFERENCES

Badrinathan, S., Shiju, T. M., Sharon Christa, A. S., Arya, R. & Pragasam, V. 2012 Purification and structural characterization of sulfated polysaccharide from *Sargassum myriocystum* and its efficacy in scavenging free radicals. *Ind. J. Pharm. Sci.* **74**, 549–555.

Bales, P. M., Renke, E. M., May, S. L., Shen, Y. & Nelson, D. C. 2013 Purification and characterization of biofilm-associated EPS exopolysaccharides from ESKAPE organisms and other pathogens. *PLoS One* **8**, e67950.

Brune, B., Dehne, N., Grossmann, N., Jung, M., Namgaladze, D., Schmid, T., von Knethen, A. & Weigert, A. 2013 Redox control of inflammation in macrophages. *Antioxid. Redox Signal.* **19**, 595–637.

CIR (Cosmetic Ingredients Review) 2012 *Safety Assessment of Microbial Polysaccharide Gums as used in Cosmetics*. CIR, Washington, DC. Available from: www.cir-safety.org/sites/default/files/microb092012rep.pdf.

Iezhitsa, I. N., Spasov, A. A., Bugaeva, L. I. & Morozov, I. S. 2002 Toxic effect of single treatment with bromantane on neurological status of experimental animals. *Bull. Exp. Biol. Med.* **133**, 380–383.

Ismail, M., Abd-Elsalam, M. A. & Morad, A. M. 1990 Do changes in body temperature following envenomation by the scorpion Leiurus quinquestriatus influence the course of toxicity? *Toxicon* **28**, 1265–1284.

Kaur, T. & Ghosh, M. 2015 Acinetobacter haemolyticus MG606 produces a novel, phosphate binding exobiopolymer. *Carbohydr. Polym.* **132**, 72–79.

Kaur, T., Ganguli, A. & Ghosh, M. 2013a Development of exobiopolymer-based biosensor for detection of phosphate in water. *Water Sci. Technol.* **68**, 2619–2625.

Kaur, T., Sharma, J., Ganguli, A. & Ghosh, M. 2013b Application of biopolymer produced from metabolic engineered

Acinetobacter sp. for the development of phosphate optoelectronic sensor. *Compos. Interf.* **21**, 143–151.

Kean, T. & Thanou, M. 2010 Biodegradation, biodistribution and toxicity of chitosan. *Adv. Drug Deliv. Rev.* **62**, 3–11.

Laine, C., Tamminen, T., Vikkula, A. & Vuorinen, T. 2002 Methylation analysis as a tool for structural analysis of wood polysaccharides. *Holzforschung* **56**, 607–614.

Meyer, J. N., Leung, M. C. K., Rooney, J. P., Sendoel, A., Hengartner, M. O., Kisby, G. E. & Bess, A. S. 2013 Mitochondria as a target of environmental toxicants. *Toxicol. Sci.* **134**, 1–17.

More, T. T., Yadav, J. S. S., Yan, S., Tyagi, R. D. & Surampalli, R. Y. 2014 Extracellular polymeric substances of bacteria and their potential environmental applications. *J. Environ. Manage.* **144**, 1–25.

Nagase, T., Mikami, T., Suzuki, S., Schuerch, C. & Suzuki, M. 1984 Lethal effect of neutral mannan fraction of bakers' yeast in mice. *Microbiol. Immunol.* **28**, 997–1007.

Necas, J. & Bartosikova, L. 2013 Carrageenan: a review. *Vet. Med.* **58**, 187–205.

Nguyen, H. T. A., Ngo, H. H., Guo, W. & Nguyen, V. T. 2012 Phosphorous removal from aqueous solutions by agricultural by-products: a critical review. *J. Water Sustain.* **2**, 193–207.

Nguyen, T. A., Ngo, H. H., Guo, W. S., Pham, T. Q., Li, F. M., Nguyen, T. V. & Bui, X. T. 2015 Adsorption of phosphate from aqueous solutions and sewage using zirconium loaded okara (ZLO): fixed-bed column study. *Sci. Total Environ.* **523**, 40–49.

Peleg, A. Y., de Breij, A., Adams, M. D., Cerqueira, G. M., Mocali, S., Galardini, M., Nibbering, P. H., Earl, A. M., Ward, D. V., Paterson, D. L., Seifert, H. & Dijkshoorn, L. 2012 The success of Acinetobacter species; genetic, metabolic and virulence attributes. *PLoS One* **7**, e46984.

Pirog, T. P., Korzh, Y. V. & Shevchuk, T. A. 2009 The effect of cultivation conditions on the physicochemical properties of the exopolysaccharide ethapolan. *Appl. Biochem. Microbiol.* **45**, 50–55.

Ramberg, J. E., Nelson, E. D. & Sinnott, R. A. 2010 Immunomodulatory dietary polysaccharides: a systematic review of the literature. *Nutr. J.* **9**, 54.

Riahi, K., Chaabane, S. & Thayer, B. B. 2014 A kinetic modeling study of phosphate adsorption onto Phoenix dactylifera L. date palm fibers in batch mode. *J. Saudi Chem. Soc.* doi:10.1016/j.jscs.2013.11.007.

Rockstrom, J., Steffen, W., Noone, K., Persson, A., Chapin, F. S., Lambin, E. F., Lenton, T. M., Scheffer, M., Folke, C., Schellnhuber, H. J., Nykvist, B., de Wit, C. A., Hughes, T., van der Leeuw, S., Rodhe, H., Sorlin, S., Snyder, P. K., Costanza, R., Svedin, U., Falkenmark, M., Karlberg, L., Corell, R. W., Fabry, V. J., Hansen, J., Walker, B., Liverman, D., Richardson, K., Crutzen, P. & Foley, J. A. 2009 A safe operating space for humanity. *Nature* **461**, 472–475.

Ruas-Madiedo, P., Medrano, M., Salazar, N., De Los Reyes-Gavilan, C. G., Perez, P. F. & Abraham, A. G. 2010 Exopolysaccharides produced by Lactobacillus and Bifidobacterium strains abrogate in vitro the cytotoxic effect of bacterial toxins on eukaryotic cells. *J. Appl. Microbiol.* **109**, 2079–2086.

Sandula, J., Kogan, G., Kacurakova, M. & Machova, E. 1999 Microbial (1 -> 3)-β-D-glucans, their preparation, physico-chemical characterization and immunomodulatory activity. *Carbohydr. Polym.* **38**, 247–253.

Satpute, S. K., Banat, I. M., Dhakephalkar, P. K., Banpurkar, A. G. & Chopade, B. A. 2010 Biosurfactants, bioemulsifiers and exopolysaccharides from marine microorganisms. *Biotechnol. Adv.* **28**, 436–450.

Sen, I. K., Mandal, A. K., Chakraborty, R., Behera, B., Yadav, K. K., Maiti, T. K. & Islam, S. S. 2014 Structural and immunological studies of an exopolysaccharide from Acinetobacter junii BB1A. *Carbohydr. Polym.* **101**, 188–195.

Singh, R. P., Jain, S. & Ramarao, P. 2013 Surfactant-assisted dispersion of carbon nanotubes: mechanism of stabilization and biocompatibility of the surfactant. *J. Nanopart. Res.* **15**, 1–19.

Terman, A., Gustafsson, B. & Brunk, U. T. 2006 The lysosomal-mitochondrial axis theory of postmitotic aging and cell death. *Chem. Biol. Interact.* **163**, 29–37.

UNEP 2012 *Global Environment Outlook-5: Environment for the Future we Want.* Progress Press Ltd, Malta.

Yang, M., Hu, X., Ning, P., Sun, W. & Ruan, T. 2011 Research progress in extracellular polymeric substances applied to biological wastewater treatment. *Ind. Water Treat.* **31**, 7–12.

First received 27 June 2016; accepted in revised form 28 August 2016. Available online 25 October 2016